J Cancer Sci Clin Ther 2021; 5 (1): 049-062 *DOI: 10.26502/jcsct.5079100*

Research Article

Integrating Routine Clinical Factors to Stratify Colorectal Cancer Patients with Liver and Lung Metastases for Immune Therapy

Friederike Schlueter[1], Katharina Doetzer[1], Martin Pruefer[1], Alexandr V. Bazhin[1,2], Jens Werner[1,2] and Barbara Mayer[1,2*]

[1]Department of General, Visceral and Transplantation Surgery, University Hospital, LMU Munich, Marchioninistraße 15, 81377 Munich, Germany

[2]German Cancer Consortium (DKTK), Partner Site Munich, Pettenkoferstraße 8a, 80336 Munich, Germany

[*]**Corresponding Author:** Dr. Barbara Mayer, Department of General, Visceral and Transplantation Surgery, University Hospital, LMU Munich, Marchioninistraße 15, 81377 Munich, Germany, Tel: +49-89-4400-76438; Fax: +49-89-4400-76433; Email: barbara.mayer@med.uni-muenchen.de

Received: 11 November 2020; **Accepted:** 15 December 2020; **Published**: 08 January 2021

Citation: Friederike Schlueter, Katharina Doetzer, Martin Pruefer, Alexandr V. Bazhin, Jens Werner, Barbara Mayer. Integrating Routine Clinical Factors to Stratify Colorectal Cancer Patients with Liver and Lung Metastases for Immune Therapy. Journal of Cancer Science and Clinical Therapeutics 5 (2021): 049-062.

Abstract

Background: Treatment with checkpoint inhibitors is approved for a small subgroup of mCRC patients with microsatellite instable high (MSI-H) or deficient microsatellite mismatch repair (dMMR) tumors indicating the strong need for additional stratification markers for immune therapy.

Patients and Methods: The immunophenotype (CD3, CD8, PD-1, PD-L1) was immunohistochemically analysed at the invasion margin (IM), the stromal (S) and intratumoral (IT) areas of 53 liver metastases (LM) and 15 lung metastases (LuM), correlated with clinical pathological parameters and statistically evaluated by the Fisher`s exact-Test (two-tailed).

Results: In LM adjuvant chemotherapy resulted in a high $CD3^+$ (p=0.011) and $CD8^+$ (p=0.02) infiltrate at the IM. Neoadjuvant chemotherapy of LM correlated with a reduced PD-L1 expression (p=0.025). LM originating from KRAS wildtype tumors demonstrated a high fraction of $CD8^+$ IT cells (p=0.038) and a strong PD-L1 expression

(p=0.03). Locally restricted LM were characterized by a high $CD8^+$ IT infiltrate (unilobular, p=0.019; maximum of 2 segments affected, p=0.038) and were found strongly PD-L1 positive (solitary LM, p=0.02; unilobular, p=0.014; ≤2 liver segments affected, p=0.018). LuM were characterized by a stronger infiltrate of $CD3^+$IT (p=0.005), $CD8^+$S (p=0.021), $CD8^+$IT (p=0.001), PD-1^+IM (p=0.007), PD-1^+S (p=0.001) and PD-1^+IT (p=0.01) compared to LM. In LuM neoadjuvant chemotherapy was accompanied by a high PD-1^+IM cell density (p=0.041). Right-sided lesions showed a high infiltrate of $CD8^+$S cells and PD-1^+IM cells (p=0.041).

Conclusion: The findings suggest previous chemotherapy, RAS status, tumor burden and sidedness as stratification markers of mCRC patients for immunotherapy, precising treatment management of distant metastases.

Keywords: Stratification parameters; Distant metastases; Immunological factors; Risk assessment; Precision immunotherapy

1. Introduction

Up to 25% [1] of the colorectal cancer (CRC) patients initially are diagnosed with synchronous liver metastasis and less frequently with lung metastasis [2-5]. In addition, despite radical surgery accompanied by drug treatment, locally advanced CRC frequently develops metachronous metastasis mostly within the first three years after first-line treatment [6, 7]. The obvious need for more efficient treatment strategies to fight metastatic CRC is reflected by an increasing number of drugs and combination therapies available. For example, recent approval was obtained for TAS-102 [8], ramucirumab [9], aflibercept [10] or regorafenib [11, 12]. Furthermore, three immunotherapy options, namely pembrolizumab [13], nivolumab and the combination nivolumab plus ipilimumab [14] are approved for metastatic colorectal cancer patients.

However, treatment with checkpoint inhibitors is restricted to the small fraction of MSI-high/dMMR selected CRC patients [15]. Currently an increasing number of predictive biomarkers independent of the MMR status for immune therapy are being discussed, such as tumor mutation burden (TMB), specific gene expression signatures, PD-L1 expression, the microbiome and immunophenotyping [16]. Nevertheless, some patients who fulfil these selection criteria do not respond to immunotherapy. Conversely, there are patients without any of these criteria revealing a good response to checkpoint inhibitors [17]. This discrepancy underscores the need of predictive factors allowing precise selection of cancer patients for immunotherapy.

In metastatic CRC most reports investigated the prognostic value of the immune microenvironment in distant metastases revealing a positive association between high densities of various immune cell phenotypes and good prognosis in both liver [18-23] and lung metastases [24, 25]. Moreover, high T-cell density in liver metastases is linked to successful chemotherapy [26]. In addition, high PD-1 expression by tumor-infiltrating lymphocytes in lung metastasis represents a rationale for the treatment of lung metastasis with checkpoint inhibitors [27]. In contrast, routine parameters to stratify patients with CRC metastases for immune therapy are rare. So far, patients receiving neoadjuvant chemotherapy [18, 20, 21, 28, 29] or presenting RAS wildtype status 30 have been identified to show a high immune infiltrate in liver metastases. Corresponding data for lung metastases is currently missing. Therefore, the aim of the present study was to identify correlations of routine clinical parameters with the

immune phenotype in distant metastases. This might help to select the most appropriate CRC patients with liver or lung metastases for immunotherapy.

2. Patients and Methods

2.1 Patient cohort

The patient cohort consists of 68 patients with metastatic colorectal cancer, receiving metastasectomy at the Department of General, Visceral, and Transplantation Surgery, Ludwig-University Hospital, LMU Munich, Munich, Germany. From each patient a liver metastasis (LM, n=53) or a lung metastasis (LuM, n=15) was analysed. Double-coded tissues and the corresponding data used in this study were provided by the Biobank of the Department of General, Visceral and Transplant Surgery in Ludwig-Maximilians-University (LMU). This Biobank operates under the administration of the Human Tissue and Cell Research (HTCR) Foundation. The framework of HTCR Foundation, which includes obtaining written informed consent from all donors, has been approved by the ethics commission of the Faculty of Medicine at the LMU (approval number 025-12) as well as the Bavarian State Medical Association (approval number 11142) in Germany.

2.2 Immunohistochemistry

Fresh tumor samples including adjacent benign reference tissue were collected according to biobanking standards. The tumor samples were immediately snap frozen in liquid nitrogen. Serial cryo-sections (5 µm) were performed using a cryotome (Leica CM 1950, Wetzler, Germany) and air dried over night at room temperature. Sections were fixed with acetone and stained immunohistochemically using the standard avidin-biotin-peroxidase complex method [31, 32]. Briefly, unspecific Fc -receptors were blocked with 10% AB-serum-DPBS (Bio-Rad; Hercules, California, USA; 805135), pH 7.4, for 20 minutes. Endogenous biotin was barred using the Avidin-/Biotin-blocking Kit (Vector Laboratories; Burlingame, California, USA; SP-2001) for 15 minutes. The primary monoclonal antibodies (mab) were incubated for one hour. The anti-CD3-mab (clone UCHT1; mouse IgG1; working concentration (wc) 1.25 µg/ml; Becton Dickenson; Franklin Lakes, New Jersey, USA; 550368) was detected with the secondary biotinylated antibody (wc 0.75 µg/ml; Jackson ImmunoResearch; West Grove, Pennsylvania, USA; 315-065-048) for 30 minutes followed by a peroxidase-conjugated streptavidin (wc 1 µg/ml; Jackson ImmunoResearch; 016-030-084) for another 30 minutes. Anti-CD8-mab (clone C8/144B; mouse IgG1; wc 3.0 µg/ml; Dako; Hamburg, Germany; M7103), anti-PD-1-mab (clone MIH4; mouse IgG1; wc 10.0 µg/ml; Affymetrix; Santa Clara, California, USA; 14-9969) and anti-PD-L1-mab (clone MIH1; mouse IgG1; wc 10.0 µg/ml; Affymetrix; 14-5983) were identified with the amplification Kit ZytoChemPlus (Zytomed Systems; Bargteheide, Germany; HRP060) according to the instructions of the manufacturer. For visualization of the antigen-antibody reaction all slides were developed in 3-amino-9-ethylcarbazol (AEC; Sigma-Aldrich; Taufkirchen, Germany; A5754) -Peroxid-solution for eight minutes. Counterstaining was performed with Mayer`s hemalum solution (Merck; Darmstadt, Germany; 109249). All incubation steps were performed in a humid chamber at room temperature. For the IgG1 isotype control the purified immunoglobulin MOPC-21 (clone MOPC-21; mouse IgG1; wc 10.0 µg/ml; Sigma-Aldrich, Germany; M5284) and for the positive control anti-CD45-mab (clone 2B11+PD7/26; mouse IgG1; wc 4.5 µg/ml; Becton Dickenson; M0701) were used. For identification of cancer cells anti-EpCAM-mab (clone BerEP4; mouse IgG1; wc 5.0 µg/ml; Dako; Hamburg, Germany; M0804) and anti-pancytokeratin-mab (clone KL1; mouse IgG1; wc 0.32 µg/ml; Zytomed Systems; MSK113) were stained.

Additionally, a standardized HE-staining was performed to estimate the percentage of cancer cells and the portion of necrosis.

2.3 Quantitative analysis of immune cells

The immune cell markers CD3, CD8 and PD-1 were quantitatively analyzed as previously described [31, 33-35]. Briefly, for each marker, three hot spot regions were chosen in three topographically different areas, namely the invasive margin (IM), the stromal (S) and intratumoral (IT) areas. The selection of the hot spot region focused on the highest density of $CD3^+$ cells identified at low magnification (50x). The IM was defined as the junction between the benign reference tissue and the tumor area according to pathological consensus guidelines [36]. Stromal leukocytes were determined as positive cells, which are in the connective tissue, without any contact to tumor cells and outside of the invasive margin. Intratumoral leukocytes were defined as positive cells which stay in close contact with tumor cells. Examples for evaluation are given in Figure 1 A-D. Three pictures were taken of each region with 200x magnification. $CD3^+$ cells and $CD8^+$ cells were examined in the same hot spot regions. For PD-1, hot spots were detected in other tumor regions.

Cell counting was done with the open source Program ImageJ. First, background was subtracted. Afterwards a colour deconvolution was performed manually by choosing three representative areas, namely background, haematoxylin and AEC-staining. An automatic threshold transferred the AEC-layer-picture into a binary picture. The watershed method was used to separate cell clusters. The absolute number of cells was counted adjusting the ´Analyze-Particle-Tool` with the values 700 to infinity for size and 0.2 to 1.0 for circularity. For the evaluation of the intratumoral cells, the area to be evaluated within the picture was additionally defined exactly with the ROI (Region of Interest)- Manager.

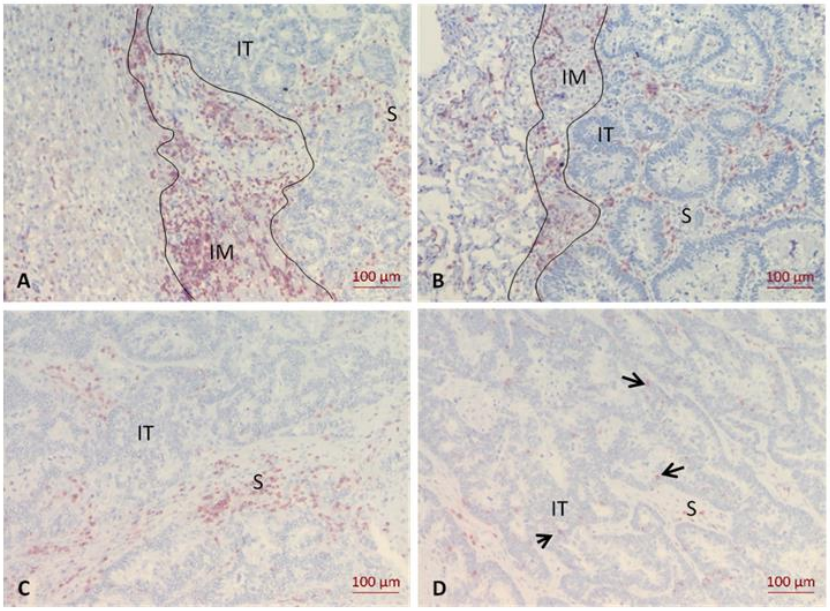

Figure 1: Immunohistochemistry of the $CD3^+$ infiltrate in liver and lung metastases. A, $CD3^+$ expression at the invasion margin (IM) of liver metastasis; B, $CD3^+$ expression at the IM of lung metastasis; C, $CD3^+$ expression in the stromal area (S) of liver metastasis; D, $CD3^+$ expression in the intratumoral area (IT) of liver metastasis. Arrows indicate individual positive cells.

2.4 Semiquantitative analyse of PD-L1

PD-L1 was expressed on tumor cells, fibroblasts and leukocytes with different intensities [37]. Therefore, the percentage of PD-L1 positive cells had to be evaluated semi-quantitatively in relation to the total amount of epithelial cells positive for EpCAM or cytokeratin and intratumoral CD45 positive immune cells. The cut off for PD-L1-positivity was ≥1% of tumor cells and intratumoral immune cells according to previous studies [38, 39].

2.5 Statistical analysis

All statistical analyses were performed with IBM SPSS v. 23 and GraphPad Prism 5. The average cell count of the three hot spots for each topographic area was calculated and then multiplied with a factor to cells/mm² for each slide and each region. Separately for each marker and each topographic area of counting, the counts of $CD3^+$, $CD8^+$ and $PD\text{-}1^+$ cells were classified in low and high by the cut-off related to the mean. Normal distribution of cell counts was determined using the Kolmogorov-Smirnov-test. Because variables were not normally distributed, the Mann-Whitney-U-Test was used to compare LM and LuM. Correlation of clinical-pathological parameters and lymphocyte counts was performed with the two-tailed Fisher's exact test. Adjuvant chemotherapy was defined as treatment of the primary tumor after its removal. Neoadjuvant chemotherapy was defined as treatment of the metastasis before surgical resection. A p-value of ≤ 0.05 was considered significant.

3. Results

3.1 Patient characteristics

A total of 68 advanced colorectal cancer patients diagnosed with liver metastasis (n=53) or lung metastasis (n=15) were included in this study. Most of the patients were initially diagnosed in an advanced UICC stage. Thus, the majority of patients received adjuvant oxaliplatin-based first line chemotherapy. Patients with a KRAS wildtype tumor more frequently developed LM (27 of 38, 71.05%) while a mutated KRAS status was often associated with LuM (6 of 9, 66.67%). Patient characteristics are summarized in detail in Table 1.

Parameters	**Location of Metastasis**					
	All Metastases		**Liver Metastases**		**Lung Metastases**	
	n	%	n	%	n	%
Patient related						
Sex						
Male	46	67.65	34	64.15	12	80
Female	22	32.35	19	35.85	3	20
Age (Years)						
Mean	63		64		59	
Median	63		64		62	
Range	30-89		30-89		37-74	
Primary Tumor Related						
Adjuvant Chemotherapy						
Yes	42	61.76	32	60.38	10	66.67
No	26	38.24	21	39.62	5	33.33

KRAS status						
Wildtype	30	63.83	27	71.05	3	33.33
Mutated	17	36.17	11	28.95	6	66.67
Missing	21		15		6	
Metastasis Related						
Grading						
G1/G2	50	79.37	39	81.25	11	73.33
G3	13	20.63	9	18.75	4	26.67
Missing	5		5		0	
Number of Metastases						
1	26	38.24	19	35.85	7	46.67
> 1	42	61.76	34	64.15	8	53.33
Diameter of the Largest Metastasis (cm)						
Mean	3.84		4.29		2.25	
Median	3.25		3.5		1.8	
Range	0.9-21.7		1.3-21.7		0.9-3.3	
Type of Metastasis						
Synchronous	35	51.47	35	66.04	0	0
Metachronous	33	48.53	18	33.6	15	100
R-Status						
R0	51	75	39	73.58	12	80
R1/R2	17	25	14	26.42	3	20
Distinction of Metastasis						
Unilobular	28	41.18	23	43.4	5	33.33
Bi-/Multilobular	40	58.82	30	56.6	10	66.67
Anatomical Site						
Left Sided	14	20.59	7	13.21	7	46.67
Right Sided	23	33.82	15	28.3	8	53.33
Both Sided	31	45.59	31	58.49		
Neoadjuvant Chemotherapy						
Yes	31	45.59	23	43.4	8	53.33
No	37	54.41	30	56.6	7	46.67

Table 1: Patient characteristics. n, number of patients.

3.2 Immune phenotype compared in colorectal liver and lung metastases

Both colorectal liver and lung metastases showed the strongest immune cell infiltrate at the invasive margin followed by the stroma. In contrast, the intratumoral fraction of immune cells was sparse. This finding was observed for $CD3^+$, $CD8^+$ and $PD\text{-}1^+$ immune cells. In all three topographic locations $CD3^+$ cells represented the highest number of leukocytes, followed by $CD8^+$ cells and $PD\text{-}1^+$ cells (Table 2, Figure 2).

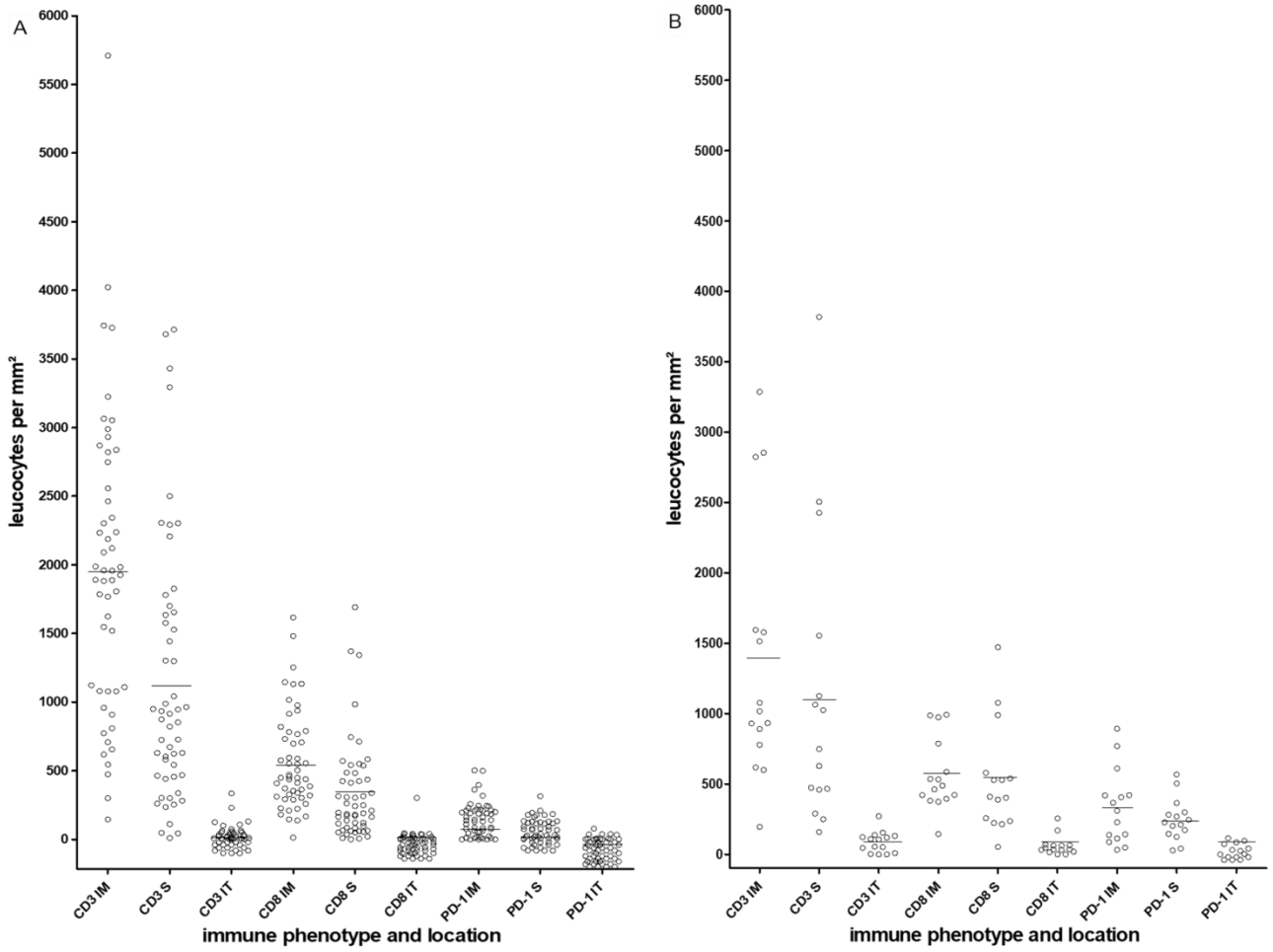

Figure 2: Heterogeneous distribution of $CD3^+$, $CD8^+$ and $PD\text{-}1^+$ cells at three topographical locations. A, liver metastases; B, lung metastases; bars represent the cut-offs (Means). Each open circle represents an individual metastatic lesion. IM, invasion margin; S, stromal; IT, intratumoral.

Comparison between liver and lung metastases revealed significant differences in the immune contexture. Lung metastases were characterised by a stronger infiltrate of $CD3^+$ IT (p=0.005), $CD8^+$ S (p=0.021), $CD8^+$ IT (p=0.001), $PD\text{-}1^+$ IM (p=0.007), $PD\text{-}1^+$ S (p=0.001) and $PD\text{-}1^+$ IT (p=0.01). In contrast liver metastases showed a stronger $CD3^+$ IM infiltrate (p=0.037) (Table 2).

		liver metastasis			lung metastasis			p-values*
Immuno Phenotype	**Location**	**n Positive/ n Analyzed**	**%**	**Mean Cell Counts (SD)**	**n Positive/ n Analyzed**	**%**	**Mean Cell Counts (SD)**	**Liver Vs. Lung**
CD3	**IM#**	52/52	100	1965 (918)	15/15	100	1379 (919)	**0.037**
	S	53/53	100	1142 (948)	15/15	100	1132 (1040)	0.923
	IT	36/53	67.9	35 (61)	13/15	86.7	87 (75)	**0.005**
CD8	**IM#**	52/52	100	558 (361)	15/15	100	565 (255)	0.539
	S	53/53	100	331 (357)	15/15	100	526 (381)	**0.021**
	IT	23/53	43.4	13 (43)	13/15	86.7	60 (68)	**0.001**
PD-1	**IM#**	47/52	90.4	144 (124)	15/15	100	332 (263)	**0.007**
	S	40/53	75.5	69 (74)	15/15	100	245 (149)	**0.001**
	IT	13/53	24.5	5 (14)	8/15	53.3	31 (41)	**0.01**

All counting performed in different topographical areas; IM, invasion margin; S, stromal; IT, intratumoral; *, Mann-Whitney-U-test was used; #, in one case the IM was not defined; n, number of samples; SD, standard deviation is given in parentheses.

Table 2: Comparison of the immune phenotypes in colorectal liver and lung metastases.

3.3 Immune infiltrate in metastatic lesions and clinicopathological parameters

The immune infiltrate in liver and lung metastases was correlated with patient related characteristics, treatment related parameters after surgery of the primary tumor and metastasis related clinical pathological parameters. All results are documented in detail in Supplementary Tables S1a-3c.

Chemotherapy, which was performed after surgery of the primary tumor, was found to have a significant modulating impact on the immune infiltrate in liver metastases. A high fraction of $CD3^+$ cells at the liver invasion front was detected after adjuvant chemotherapy ($CD3^+$ IM high: 19 out of 31, 61.29%). In contrast, in chemo-naive liver metastases the number of $CD3^+$ cells was low ($CD3^+$ IM low: 16 out of 21, 76.19%; p=0.011). Similar, $CD8^+$ cells were enriched at the invasion front after first-line chemotherapy ($CD8^+$ IM high: 16 out of 30, 53.33%), but were low if no chemotherapy was performed ($CD8^+$ IM low: 18 out of 22, 81.81%; p=0.02). The increase of the immune infiltrate was independent of the type of adjuvant drug treatment. No difference was found between oxaliplatin-based, irinotecan-based and antibody-based treatment in this small cohort. Interestingly, all but two (eight of ten cases, 80%) metachronous liver metastases, which received an adjuvant treatment, revealed a high $CD3^+$ infiltrate at the IM, despite a long progression free interval (mean 24.8 months, range >6 to 77 months).

The treatment decision factor KRAS was found to correlate with the extent of the $CD8^+$ IT infiltrate. Liver metastases originating from KRAS wildtype primary tumors often exposed a high $CD8^+$ infiltrate within the tumor nests

($CD8^+$ IT high: 9 out of 27, 33.33%). Conversely, all KRAS mutated tumors (n=11) showed a low density of $CD8^+$ IT cells (p=0.038).

Correlation with metastasis related clinical pathological parameters revealed a significant association between the extent of the immune cell infiltrate and the tumor burden. Unilobular liver metastases showed a high $CD8^+$ IT infiltrate ($CD8^+$ IT high: 9 out of 23, 39.13%), while in liver metastases involving both lobes the $CD8^+$ IT infiltrate was low ($CD8^+$ IT low: 27 out of 30, 90%; p=0.019). Similarly, liver metastases with a maximum of two affected segments ($CD8^+$ IT high: 7 out of 17, 41.18%) were characterized by a strong $CD8^+$ IT infiltrate. Conversely, the number of $CD8^+$ IT cells in liver metastases with more than two segments involved was low ($CD8^+$ IT low: 31 out of 36, 86.11%; p=0.038).

In the small cohort of metachronous lung metastases a significant correlation was found between right-sided lung metastasis and a high $CD8^+$ S infiltrate ($CD8^+$ S high: 6 out of 8, 75%). Left-sided lung metastases on the other hand showed a low fraction of $CD8^+$ S cells ($CD8^+$ S low: 6 out of 7, 85.71%; p=0.041). Sidedness dependency was also observed for the PD-1 infiltrate. Right-sided lung metastases showed a high fraction of $PD\text{-}1^+$ cells at the invasive margin, which stood in contrast to left-sided lesions (p=0.041). In addition, $PD\text{-}1^+$ cell density at the invasive margin of lung metastases was high following neoadjuvant chemotherapy, which differed from the low $PD\text{-}1^+$ infiltrate in lung metastasis without previous treatment (p=0.041).

3.4 PD-L1 expression in liver and lung metastasis

High PD-L1 expression was found in 24 out of 53 (45.28%) liver metastases and in 13 out of 15 (86.67%) lung metastases. Strong PD-L1 expression in liver metastases was accompanied by a strong T cell infiltrate at the invasive margin ($CD3^+$ IM, p=0.05; $CD8^+$ IM, p=0.002; $PD\text{-}1^+$ IM, p=0.025), in the stroma ($PD\text{-}1^+$ S, p=0.014) and the intratumoral area ($CD3^+$ IT, p=0.002; $CD8^+$ IT, p=0.024; $PD\text{-}1^+$ IT, p=0.017; Supplementary Table S4). Liver metastases originating from KRAS wildtype primary CRC were identified PD-L1 positive (13 out of 27, 48.15%), while liver metastases with a KRAS mutated phenotype showed no PD-L1 expression (10 out of 11, 90.91%; p=0.03). In addition, high PD-L1 expression correlated with limited tumor load (1 liver metastases involved, p=0.02; unilobular liver metastasis, p=0.014; ≤2 liver segments affected, p=0.018). After neoadjuvant chemotherapy a reduced PD-L1 expression was observed in liver metastases (17 out of 23, 73.91%), whereas liver metastases without previous chemotherapy were characterized by a high PD-L1 expression (18 out of 30, 60%; p=0.025). No significant associations were found in the small cohort of lung metastases. The results of all correlations are summarized in Supplementary Table S5.

4. Discussion

The clinical-pathological relevance of the immune phenotype and the topographic distribution of the intrametastatic immune infiltrate was immunohistochemically analyzed in 53 liver metastases and 15 lung metastases of CRC. In both metastatic locations $CD3^+$, $CD8^+$ and $PD\text{-}1^+$ lymphocytes were detected in a high fraction at the invasive margin, and to a lesser extend in the stromal area. In contrast, intratumoral immune cells were rare. Correlation with routine clinical pathological factors identified a significant accumulation of $CD3^+$ and $CD8^+$ T-cells at the invasive margin of liver metastases after adjuvant chemotherapy. High density values of $CD3^+$ cells and $CD8^+$ cells were found independent of the

substance class used in the adjuvant treatment. Chemotherapy can provide broad-acting immune stimulating effects such as T-cell priming and recruitment [40]. Indeed, in the neoadjuvant setting oxaliplatin-based and anti-EGFR-based treatments strongly enhanced the immune infiltrate in liver metastatic lesions [30, 41]. These results indicate that standard of care therapy might induce neo-antigen expression elevating cancer immunogenicity [42]. Considering the large number of deviations in the clinical chemotherapeutic settings, the correlation between the extent of drug treatment and the extend of the $CD3^+$ and $CD8^+$ infiltrate needs to be further analyzed in preclinical models. In addition, chemotherapy might result at least in part in a less immune suppressive microenvironment allowing surrounding T-cells to infiltrate [26]. However, successful immunotherapy, for example treatment with bispecific antibodies [43], checkpoint-inhibitors [44] or CAR T-cells [45, 46] require immediate proximity between cancer cells and leukocytes. Therefore re-direction of the leukocytes from the invasive margin into the tumor nests is necessary and might be stimulated by additional therapeutics such as GM-CSF or CCL5 [47-49].

Correlation between the immunological factors and the extent of the liver metastatic disease revealed that high intratumoral infiltrates of $CD8^+$ cells and a high PD-L1 expression were more frequently observed in patients diagnosed with restricted liver metastases reflecting less aggressive metastatic behaviour. This finding suggests that $CD8^+$ cells might control tumor spread [50].

Furthermore, a subgroup of liver metastases originating from KRAS wildtype cancers was identified strongly PD-L1 positive. Simultaneous expression of two drugable targets suggests a biomarker driven patient stratification for dual inhibition combining a checkpoint-inhibitor with an anti-EGFR inhibitor. Indeed, there are currently several ongoing trials, namely the AVETUX study (NCT03174405) and CAVE study (EudraCT: 2017-004392-32) combining Cetuximab and Avelumab treatment. These significant correlations suggest adjuvant chemotherapy, KRAS wildtype and limited tumor burden as new stratification markers for colorectal liver metastasis characterized by a strong leukocyte infiltrate.

In addition to the liver metastases, immune phenotyping was performed in a small cohort of lung metastases. Significant differences in the immune contexture were identified between liver and lung metastases. Lung metastases revealed a significant stronger infiltrate of CD3, CD8 and PD-1 positive cells in both, the stromal and intratumoral compartment. This finding shows that lung metastases can be an attractive target for immune therapy.

In the present study, right-sided lung metastases showed a higher $CD8^+$ infiltrate in the stroma and $PD\text{-}1^+$ infiltrate at the invasion margin compared to left-sided lung metastases. Interestingly, it is known that patients with right-sided lung metastases have a better prognosis [51]. These results suggest immunological differences depending on the anatomical site of metastatic lesions similar as published for right-sided and left-sided primary colorectal cancer [52-55].

Correlation with therapeutic variables revealed a significant correlation between performance of neoadjuvant second-line chemotherapy and a high PD-1 infiltrate at the invasion margin. This finding supports chemotherapy as a precondition for immunotherapy not only in liver metastases but also in lung metastases of colorectal cancer. In contrast to LM, sidedness of metastasis and neoadjuvant treatment were identified as additional selection parameters for immunotherapy of LuM.

Moreover, lung metastases were observed more frequently PD-L1 positive compared to liver metastases. This finding supports treatment of colorectal lung metastasis with checkpoint inhibitors similar as reported for the standard therapy of non-small-cell lung cancer. The biological differences reported for the first time between liver and lung metastases might result in different treatment strategies of the CRC metastatic lesions. However, the results obtained in the present pilot study need to be confirmed in an enlarged cohort.

5. Conclusion

In conclusion, this pilot study identified differences of the immune contexture between liver and lung metastases of colorectal cancer. Most important, lung metastases revealed higher counts of intratumoral $CD3^+$, $CD8^+$ and $PD\text{-}1^+$ cells and a more frequent PD-L1 expression. This indicates that lung metastases are appropriate for immunotherapy. Routine clinical pathological parameters were identified as patient stratification markers for immunotherapy, i.e. KRAS status, tumor burden in liver metastases, sidedness of lung metastases and previous chemotherapy in both metastatic lesions. Thus, in addition to the known biological indicators, namely the MSI/MSS status, the PD-L1 status and the extent of lymphocyte infiltration [55], these clinical factors are suggested to be involved in precision immunotherapy. Based on these results, new treatment strategies can be proposed, specifically combination schemes of immunotherapy with EGFR inhibition and sequential treatment of chemotherapy with subsequent checkpoint inhibition.

Acknowledgments

We thank the staff members of the Biobank (Head: PD Dr. med. T. Schiergens) especially Maresa Demmel, Nadine Gesse, Ute Bossmanns and Beatrice Rauter for tissue sample/data organization, Michael Pohr for technical support and Robin v. Holzschuher for providing language help. This work was supported by the German Federal Ministry of Education and Research, Leading Edge Cluster m4 (B.M.) under Grant FKZ 16EX1021N.

Conflict of Interest Disclosure Statement

The authors declare no potential conflicts of interest.

References

1. Okholm C, Mollerup TK, Schultz NA, Strandby RB, Achiam MP. Synchronous and metachronous liver metastases in patients with colorectal cancer. Dan Med J (2018): 65.
2. Robinson JR, Newcomb PA, Hardikar S, Cohen SA, Phipps AI. Stage IV colorectal cancer primary site and patterns of distant metastasis. Cancer epidemiology (2017): 48:92-95.
3. Adam R, de Gramont A, Figueras J, et al. Managing synchronous liver metastases from colorectal cancer: a multidisciplinary international consensus. Cancer treatment reviews 41 (2015): 729-741.
4. Riihimaki M, Hemminki A, Sundquist J, Hemminki K. Patterns of metastasis in colon and rectal cancer. Scientific reports 6 (2016): 29765.
5. Holch JW, Demmer M, Lamersdorf C, et al. Pattern and Dynamics of Distant Metastases in Metastatic Colorectal Cancer. Visceral medicine 33 (2017): 70-75.
6. Fournel L, Maria S, Seminel M, et al. Prognostic factors after pulmonary metastasectomy of colorectal cancers: a single-center experience. Journal of thoracic disease 9 (2017): S1259-s1266.
7. D'Angelica M, Kornprat P, Gonen M, et al. Effect on outcome of recurrence patterns after hepatectomy for

colorectal metastases. Annals of surgical oncology 18 (2011): 1096-1103.

8. European Medicines Agency. EPAR summary for the public - trifluridine/tipiracil (2018).
9. European Medicines Agency. EPAR summary for the public – Ramucirumab (2018).
10. European Medicines Agency. EPAR summary for the public – Aflibercept (2018).
11. European Medicines Agency. EPAR summary for the public – regorafenib (2018).
12. Hopirtean C, Nagy V. Optimizing the use of anti VEGF targeted therapies in patients with metastatic colorectal cancer: review of literature. Clujul medical 91 (2018): 12-17.
13. Boyiadzis MM, Kirkwood JM, Marshall JL, et al. Significance and implications of FDA approval of pembrolizumab for biomarker-defined disease. J Immunother Cancer 6 (2018): 35.
14. Overman MJ, Lonardi S, Wong KYM, et al. Durable Clinical Benefit With Nivolumab Plus Ipilimumab in DNA Mismatch Repair-Deficient/Microsatellite Instability-High Metastatic Colorectal Cancer. Journal of clinical oncology: official journal of the American Society of Clinical Oncology 36 (2018): 773-779.
15. Le DT, Uram JN, Wang H, et al. PD-1 Blockade in Tumors with Mismatch-Repair Deficiency. N Engl J Med 372 (2015): 2509-2520.
16. Arora S, Velichinskii R, Lesh RW, et al. Existing and Emerging Biomarkers for Immune Checkpoint Immunotherapy in Solid Tumors. Adv Ther 36 (2019): 2638-2678.
17. De Toni EN, Roessler D. Using dual checkpoint blockade to treat fibrolamellar hepatocellular carcinoma. Gut (2020).
18. Katz SC, Bamboat ZM, Maker AV, et al. Regulatory T cell infiltration predicts outcome following resection of colorectal cancer liver metastases. Annals of surgical oncology 20 (2013): 946-955.
19. Berthel A, Zoernig I, Valous NA, et al. Detailed resolution analysis reveals spatial T cell heterogeneity in the invasive margin of colorectal cancer liver metastases associated with improved survival. Oncoimmunology 6 (2017): e1286436.
20. Mlecnik B, Van den Eynde M, Bindea G, et al. Comprehensive Intrametastatic Immune Quantification and Major Impact of Immunoscore on Survival. Journal of the National Cancer Institute (2018): 110.
21. Van den Eynde M, Mlecnik B, Bindea G, et al. The Link between the Multiverse of Immune Microenvironments in Metastases and the Survival of Colorectal Cancer Patients. Cancer cell 34 (2018): 1012-1026. e1013.
22. Wang Y, Lin HC, Huang MY, et al. The Immunoscore system predicts prognosis after liver metastasectomy in colorectal cancer liver metastases. Cancer Immunol Immunother 67 (2018): 435-444.
23. Hof J, Kok K, Sijmons RH, de Jong KP. Systematic Review of the Prognostic Role of the Immune System After Surgery of Colorectal Liver Metastases. Front Oncol 9 (2019): 148.
24. Remark R, Alifano M, Cremer I, et al. Characteristics and clinical impacts of the immune environments in colorectal and renal cell carcinoma lung metastases: influence of tumor origin. Clinical cancer research: an official journal of the American Association for Cancer Research 19 (2013): 4079-4091.
25. Schweiger T, Berghoff AS, Glogner C, et al. Tumor-infiltrating lymphocyte subsets and tertiary lymphoid structures in pulmonary metastases from colorectal cancer. Clinical and experimental metastasis (2016).

26. Halama N, Michel S, Kloor M, et al. Localization and density of immune cells in the invasive margin of human colorectal cancer liver metastases are prognostic for response to chemotherapy. Cancer Res 71 (2011): 5670-5677.
27. Kollmann D, Schweiger T, Schwarz S, et al. PD1-positive tumor-infiltrating lymphocytes are associated with poor clinical outcome after pulmonary metastasectomy for colorectal cancer. Oncoimmunology 6 (2017): e1331194.
28. D'Alterio C, Nasti G, Polimeno M, et al. CXCR4-CXCL12-CXCR7, TLR2-TLR4, and PD-1/PD-L1 in colorectal cancer liver metastases from neoadjuvant-treated patients. Oncoimmunology 5 (2016): e1254313.
29. Dosset M, Vargas TR, Lagrange A, et al. PD-1/PD-L1 pathway: an adaptive immune resistance mechanism to immunogenic chemotherapy in colorectal cancer. Oncoimmunology 7 (2018): e1433981.
30. Ledys F, Klopfenstein Q, Truntzer C, et al. RAS status and neoadjuvant chemotherapy impact CD8+ cells and tumor HLA class I expression in liver metastatic colorectal cancer. J Immunother Cancer 6 (2018): 123.
31. Dotzer K, Schluter F, Schoenberg MB, et al. Immune Heterogeneity Between Primary Tumors and Corresponding Metastatic Lesions and Response to Platinum Therapy in Primary Ovarian Cancer. Cancers (Basel) (2019): 11.
32. Mayer B, Lorenz C, Babic R, et al. Expression of leukocyte cell adhesion molecules on gastric carcinomas: possible involvement of LFA-3 expression in the development of distant metastases. International journal of cancer 64 (1995): 415-423.
33. Vayrynen JP, Vornanen JO, Sajanti S, et al. An improved image analysis method for cell counting lends credibility to the prognostic significance of T cells in colorectal cancer. Virchows Archiv: an international journal of pathology 460 (2012): 455-465.
34. Miksch RC, Hao J, Schoenberg MB, et al. Development of a reliable and accurate algorithm to quantify the tumor immune stroma (QTiS) across tumor types. Oncotarget 8 (2017): 114935-114944.
35. Schoenberg MB, Hao J, Bucher JN, et al. Perivascular Tumor-Infiltrating Leukocyte Scoring for Prognosis of Resected Hepatocellular Carcinoma Patients. Cancers (Basel) (2018): 10.
36. van Dam PJ, van der Stok EP, Teuwen LA, et al. International consensus guidelines for scoring the histopathological growth patterns of liver metastasis. Br J Cancer 117 (2017): 1427-1441.
37. Zerdes I, Matikas A, Bergh J, et al. Genetic, transcriptional and post-translational regulation of the programmed death protein ligand 1 in cancer: biology and clinical correlations. Oncogene (2018).
38. Korehisa S, Oki E, Iimori M, et al. Clinical significance of programmed cell death-ligand 1 expression and the immune microenvironment at the invasive front of colorectal cancers with high microsatellite instability. International journal of cancer 142 (2018): 822-832.
39. Jomrich G, Silberhumer GR, Marian B, et al. Programmed death-ligand 1 expression in rectal cancer. European surgery: ACA: Acta chirurgica Austriaca 48 (2016): 352-356.
40. Opzoomer JW, Sosnowska D, Anstee JE, et al. Cytotoxic Chemotherapy as an Immune Stimulus: A Molecular Perspective on Turning Up the Immunological Heat on Cancer. Front Immunol 10 (2019): 1654.
41. Inoue Y, Hazama S, Suzuki N, et al. Cetuximab strongly enhances immune cell infiltration into liver

metastatic sites in colorectal cancer. Cancer science 108 (2017): 455-460.

42. Ward JP, Gubin MM, Schreiber RD. The Role of Neoantigens in Naturally Occurring and Therapeutically Induced Immune Responses to Cancer. Adv Immunol 130 (2016): 25-74.
43. Kobold S, Pantelyushin S, Rataj F, et al. Rationale for Combining Bispecific T Cell Activating Antibodies With Checkpoint Blockade for Cancer Therapy. Front Oncol 8 (2018): 285.
44. Tintelnot J, Stein A. Immunotherapy in colorectal cancer: Available clinical evidence, challenges and novel approaches. World J Gastroenterol 25 (2019): 3920-3928.
45. Gutting T, Burgermeister E, Hartel N, et al. Checkpoints and beyond-Immunotherapy in colorectal cancer. Semin Cancer Biol 55 (2019): 78-89.
46. Miliotou AN, Papadopoulou LC. CAR T-cell Therapy: A New Era in Cancer Immunotherapy. Curr Pharm Biotechnol 19 (2018): 5-18.
47. Wei XX, Chan S, Kwek S, et al. Systemic GM-CSF Recruits Effector T Cells into the Tumor Microenvironment in Localized Prostate Cancer. Cancer Immunol Res 4 (2016): 948-958.
48. Zhang S, Zhong M, Wang C, et al. CCL5-deficiency enhances intratumoral infiltration of CD8(+) T cells in colorectal cancer. Cell Death Dis 9 (2018): 766.
49. van der Woude LL, Gorris MAJ, Halilovic A, et al. Migrating into the Tumor: a Roadmap for T Cells. Trends in cancer 3 (2017): 797-808.
50. Tsukumo SI, Yasutomo K. Regulation of CD8(+) T Cells and Antitumor Immunity by Notch Signaling. Front Immunol 9 (2018): 101.
51. Ampollini L, Gnetti L, Goldoni M, et al. Pulmonary metastasectomy for colorectal cancer: analysis of prognostic factors affecting survival. Journal of thoracic disease 9 (2017): S1282-s1290.
52. Zhao Y, Ge X, He J, et al. The prognostic value of tumor-infiltrating lymphocytes in colorectal cancer differs by anatomical subsite: a systematic review and meta-analysis. World J Surg Oncol 17 (2019): 85.
53. Berntsson J, Svensson MC, Leandersson K, et al. The clinical impact of tumour-infiltrating lymphocytes in colorectal cancer differs by anatomical subsite: A cohort study. International journal of cancer 141 (2017): 1654-1666.
54. Berntsson J, Eberhard J, Nodin B, et al. Expression of programmed cell death protein 1 (PD-1) and its ligand PD-L1 in colorectal cancer: Relationship with sidedness and prognosis. Oncoimmunology 7 (2018): e1465165.
55. Le DT, Hubbard-Lucey VM, Morse MA, et al. A Blueprint to Advance Colorectal Cancer Immunotherapies. Cancer Immunol Res 5 (2017): 942-949.